Sphingosine-1-Phosphate as an Amphipathic Metabolite: Its Properties in Aqueous and Membrane Environments

Marcos García-Pacios,[†‡] M. Isabel Collado,[§] Jon V. Busto,[†‡] Jesús Sot,[†‡] Alicia Alonso,[†‡] José-Luis R. Arrondo,[†‡] and Félix M. Goñi[†‡*]

[†]Unidad de Biofísica (CSIC-UPV/EHU), [‡]Departamento de Bioquímica, and [§]Servicio General de Resonancia Magnética Nuclear, Universidad del País Vasco, Bilbao, Spain

ABSTRACT Sphingosine-1-phosphate (S1P) is currently considered to be an important signaling molecule in cell metabolism. We studied a number of relevant biophysical properties of S1P, using mainly Langmuir balance, differential scanning calorimetry, ^{31}P-NMR, and infrared (IR) spectroscopy. We found that, at variance with other, structurally related sphingolipids that are very hydrophobic, S1P may occur in either an aqueous dispersion or a bilayer environment. S1P behaves in aqueous media as a soluble amphiphile, with a critical micelle concentration of $\approx 12\ \mu$M. Micelles give rise to larger aggregates (in the micrometer size range) at and above a 1 mM concentration. The aggregates display a thermotropic transition at ~60°C, presumably due to the formation of smaller structures at the higher temperatures. S1P can also be studied in mixtures with phospholipids. Studies with dielaidoylphosphatidylethanolamine (DEPE) or deuterated dipalmitoylphosphatidylcholine (DPPC) show that S1P modifies the gel-fluid transition of the glycerophospholipids, shifting it to lower temperatures and decreasing the transition enthalpy. Low (<10 mol %) concentrations of S1P also have a clear effect on the lamellar-to-inverted hexagonal transition of DEPE, i.e., they increase the transition temperature and stabilize the lamellar versus the inverted hexagonal phase. IR spectroscopy of natural S1P mixed with deuterated DPPC allows the independent observation of transitions in each molecule, and demonstrates the existence of molecular interactions between S1P and the phospholipid at the polar headgroup level that lead to increased hydration of the carbonyl group. The combination of calorimetric, IR, and NMR data allowed the construction of a temperature-composition diagram ("partial phase diagram") to facilitate a comparative study of the properties of S1P and other related lipids (ceramide and sphingosine) in membranes. In conclusion, two important differences between S1P and ceramide are that S1P stabilizes the lipid bilayer structure, and physiologically relevant concentrations of S1P can exist dispersed in the cytosol.

INTRODUCTION

Over the past decade, a whole family of sphingosine-related molecules have been recognized as intracellular metabolic signals. One such molecule is sphingosine-1-phosphate (S1P), which is now widely accepted as a bioactive lipid that regulates important physiological functions (1–3). It can be generated intracellularly, serving as a second messenger for cell proliferation (4,5) and survival (suppression of apoptosis) (6). S1P can also stimulate aldosterone secretion in adrenal gland cells (7). This sphingolipid interacts with specific G-protein-coupled receptors (S1P1-S1P5 receptors) at the plasma membrane of cells. Binding of S1P to S1P1 regulates chemotaxis and new blood vessel formation (angiogenesis), whereas activation of S1P5, and possibly S1P3, receptors leads to rounding and neurite retraction (8). S1P2 and S1P3 receptors play a major role in mediating cardioprotection from ischemia/reperfusion injury in vivo (9). S1P receptors are also important in the regulation and protection of biological barriers (10), and the S1P receptor signaling system may provide a target for the therapy of multiple sclerosis (8). Some of these effects appear to be related to S1P's capacity to induce extensive cytoskeletal rearrangements (3). S1P is also involved in Ca^{2+}-dependent signaling in yeast and higher plants (11).

Because of its lipidic nature, S1P must exert its regulatory role essentially at the membrane level, as is the case for ceramides and other related lipids (12). Moreover, because of its amphiphilic nature, S1P gives rise to stable dispersions in water. This makes an analysis of the physical properties of S1P in both aqueous dispersions and mixtures with the major components of membrane bilayers (i.e., the glycerophospholipids) pertinent. In this study we used a combination of techniques—mainly Langmuir balance, differential scanning calorimetry (DSC), ^{31}P-NMR, and infrared (IR) spectroscopy—to explore the properties of fully hydrated pure S1P and its effects on the gel-fluid and lamellar-to-inverted hexagonal phase transitions of dielaidoylphosphatidylethanolamine (DEPE), a glycerophospholipid that exhibits both transitions within a convenient temperature range (37.5°C and 65°C, respectively) when dispersed in water in the pure state. In addition, the use of perdeuterated fatty acyl-chain dipalmitoylphosphatidylcholine (d_{62}-DPPC) in combination with IR spectroscopy has allowed the independent study of the behavior of S1P and DPPC in a mixture of both lipids (13). Such measurements indicate that S1P exerts clear effects on the phospholipid phase transitions, particularly on the lamellar-hexagonal transition of DEPE. Moreover, S1P occurs in a monomer-micelle equilibrium in water, and, as a consequence, it is the only sphingolipid signaling molecule that can be found dissociated from the cell membranes in the cytosol.

Submitted May 12, 2009, and accepted for publication July 1, 2009.

*Correspondence: felix.goni@ehu.es

Editor: Michael Edidin.

0006-3495/09/09/1398/10 $2.00

doi: 10.1016/j.bpj.2009.07.001

MATERIALS AND METHODS

Materials

DEPE, d_{62}-DPPC, and S1P were supplied by Avanti Polar Lipids (Alabaster, AL). The lipids were codissolved in ethanol, and the mixture was evaporated to dryness under a stream of nitrogen. Traces of solvent were removed by evacuating the samples under high vacuum overnight. The resulting lipid films were hydrated in a D_2O buffer consisting of 20 mM PIPES, 150 mM NaCl, 1 mM EDTA, pH 7.4, and kept for 1 h at 45°C with stirring. 1,1′-Dioctadeyl-3,3,3′,3′-tetramethylindo-carbocyanine perchlorate (DiI) was obtained from Invitrogen (Eugene, OR).

Critical micelle concentration

The critical micelle concentration (CMC) of S1P was estimated (14) on the basis of measurements of surface pressure in S1P dispersions. The surface properties of monomolecular S1P layers at the air-water interface were studied with the use of μTrough-S equipment (Kibron, Helsinki, Finland) at 25°C under constant stirring and a constant monolayer area of 3.14 cm^2. The aqueous subphase consisted of 1 mL 20 mM PIPES, 150 mM NaCl, 1 mM EDTA, pH 7.4. S1P (in <50 μL buffer) was injected into the subphase with a Hamilton microsyringe through a hole connected to the subphase.

Confocal fluorescence microscopy

S1P suspensions in concentrations of 0.03–2.76 mM, containing 0.2 mol % DiI, were examined in an inverted confocal fluorescence microscope (Nikon D-ECLIPSE C1; Nikon, Melville, NY). The excitation wavelength for DiI was 561 nm. The images were collected using band-pass filters of 593 ± 20 nm. These experiments were performed at 25–28°C. Image treatment was performed using the software EZ-C1 3.20 (Nikon).

DSC

For DSC, both the lipid suspension and buffer were degassed before being loaded into the sample or reference cell of an MC-2 high-sensitivity scanning calorimeter (MicroCal, Northampton, MA). The final DEPE concentration was 0.4 mM for samples in which gel-to-fluid transitions were measured, and 7 mM for those in which fluid-to-inverted hexagonal transitions were studied. Three heating scans, and occasionally a cooling one, at 45°C/h were recorded for each sample. After the first one, successive heating scans on the same sample always yielded superimposable thermograms. Transition temperatures, enthalpies, and widths at half-height were determined using the software ORIGIN (MicroCal) provided with the calorimeter.

IR spectroscopy

IR spectra were recorded in a Nicolet Magna II 550 spectrometer (Thermo Scientific, Waltham, MA) equipped with a mercury cadmium telluride detector. Lipid mixtures were resuspended in buffer at a constant S1P concentration of 80 mM, so that in samples with d_{62}-DPPC the total lipid concentration was correspondingly increased. Samples were placed in a temperature-regulated Harrick cell (Ossining, NY) equipped with CaF_2 windows and 50-μm spacers. Samples were heated at a constant rate of 60°C/h, and 304 scans/°C were acquired with a nominal resolution of 2 cm^{-1} using Omnic (Nicolet) rapid-scan software. Band maxima were determined from derivative spectra, and Fourier derivation was performed with a power of 3 and a breakpoint of 0.3.

Light scattering

The suspension static light scattering was measured in an SLM-AMINCO 8100 spectrofluorometer (Horiba Jobin Yvon, Edison, NJ) at room temperature, with excitation and emission wavelengths set at 400 nm.

NMR spectra

^{31}P-NMR spectra were recorded in a Bruker (Rheinstetten, Germany) AV500 spectrometer operating at 500 MHz for protons (202.4 MHz for ^{31}P). The final phospholipid concentration was 100 mM. Spectral parameters were 45° pulses (11.5 μs), pulse interval = 1 s, sweep width = 30 kHz, and full proton decoupling. Two thousand free induction decays were routinely accumulated from each sample, and the spectra were plotted with a line-broadening of 40 Hz. Samples were equilibrated for at least 10 min at each temperature before data were acquired.

RESULTS

S1P in aqueous suspensions

The chemical structure of S1P suggests an amphipathic nature. Consequently, a monomer-aggregate equilibrium in aqueous media should be expected. We tested this by studying the surface pressure properties of S1P in the Langmuir balance (Fig. 1 *A*). The concentration-dependent increase in

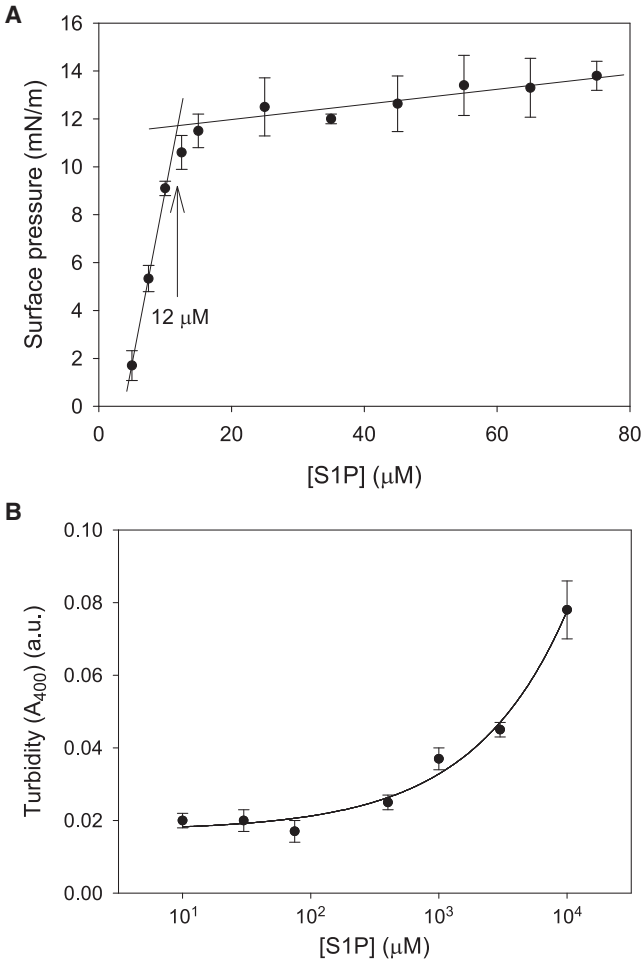

FIGURE 1 (*A*) CMC of S1P estimated by the surface-pressure method. S1P in PIPES buffer, pH 7.4 (see Materials and Methods), at 21°C. The CMC was measured as the point beyond which further increases in S1P concentration do not lead to increased surface pressures. Average values ± SE of the mean ($n = 3$). (*B*) Turbidity (absorbance at 400 nm) of S1P suspensions in PIPES buffer, pH 7.4, at 21°C as a function of S1P concentration. Average values ± SE of the mean ($n = 4$).

surface pressure confirms the amphipathic properties of this lipid. Beyond ≈ 12 μM, increasing S1P concentrations hardly cause any further increase in surface pressure. This is usually taken as an indication that, above this concentration, surfactant monomers begin to aggregate, giving rise to micelles (i.e., 12 μM is the CMC of S1P in PIPES buffer, pH 7.4, at 21°C). This is rather close to the value (≈ 14 μM) recently found by Sasaki et al. (15) using NMR spectroscopy under similar conditions.

Furthermore, turbidity (A_{400}) measurements of S1P suspensions indicated a concentration-dependent increase in suspension turbidity that was particularly marked at and above 1 mM lipid (Fig. 1 *B*). This should be an indication of an aggregation process beyond micelle formation. Confocal fluorescence microscopy of 2.76 mM S1P suspensions confirmed the presence of amorphous aggregates in the micrometer size range (Fig. 2). Such structures are rarely seen at 70 μM S1P, and they are not detected at 30 μM (pictures not shown).

Aggregates of amphiphiles containing long aliphatic chains often exhibit thermotropic order-disorder phase transitions in a temperature range close to the mammalian physiological temperature. A DSC study of 10 μM S1P in buffer revealed an endothermic signal centered at 65.0°C (Fig. 3). The transition width at midheight was of 4.4°C, and the transition enthalpy was of 340 cal/mol lipid, i.e., one order of magnitude smaller than that of the saturated glycerophospholipids (16).

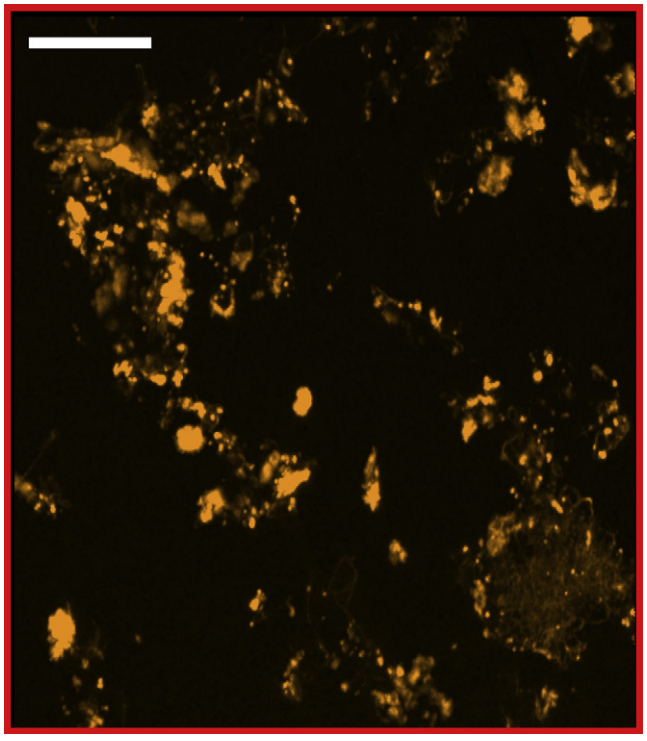

FIGURE 2 Confocal fluorescence microscopy of a 2.76 mM suspension of S1P. The lipid was doped with 0.2 mol % DiI. Bar = 10 μm.

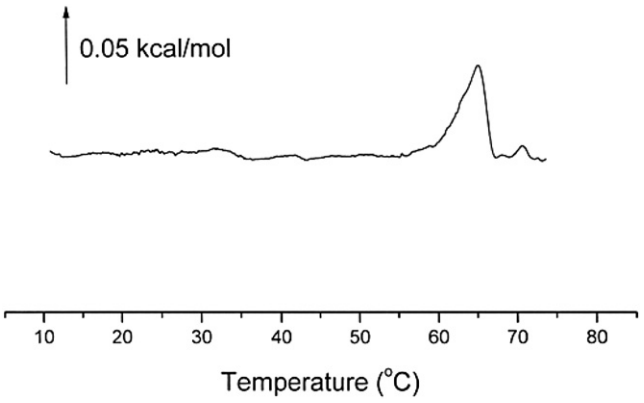

FIGURE 3 DSC of S1P in buffer dispersion. Second heating scan. The S1P concentration was 10 mM.

The thermal behavior of S1P aggregates in aqueous media was further explored by IR spectroscopy in the 20–80°C temperature range. The CH_2 stretching vibration bands of

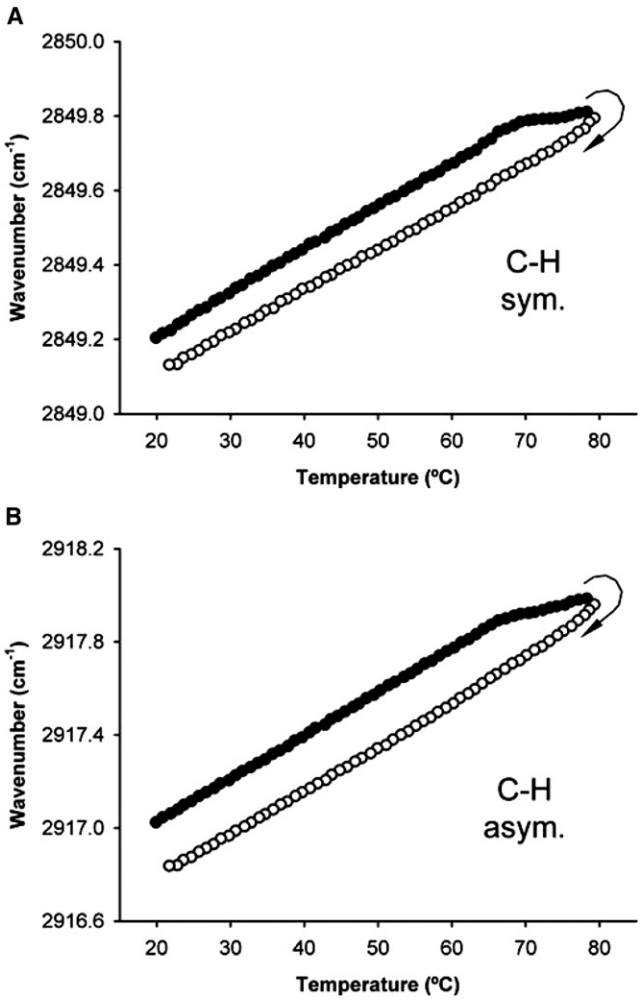

FIGURE 4 Band positions (maximal frequencies) of the C-H stretching vibrations of S1P as a function of temperature. (*A*) Symmetric stretching. (*B*) Asymmetric stretching. (•) Heating run. (○) Cooling run.

lipids have been used very often in the detection of phase transitions. In general, thermotropic phase transitions lead to more disordered chains, as indicated by a shift of CH_2 stretching vibration bands to higher wavenumbers (lower frequencies) (17,18). The behavior of S1P CH_2 asymmetric and symmetric stretching vibration bands is shown in Fig. 4. At 20°C the asymmetric band had a maximum at 2917 cm^{-1} that in the case of saturated phosphatidylcholines would correspond to a predominantly *anti* methylene chain conformation, as seen in the gel phase (18). Heating up the sample caused a gradual increase in wavenumber, compatible with an increased chain disorder. Maximum wavenumbers increased linearly with temperature up to 65°C, above which the wavenumbers continued to increase, albeit with a lower slope. Cooling back from 80°C to 20°C showed hysteresis, which is unusual in the gel-fluid transitions of phospholipids. A change in slope was also detected at 65°C for the P-O stretching band at 1089 cm^{-1}, with hysteresis being equally observed (Fig. 5 *A*). However, no such changes were seen in the thermal behavior of the CH_2 bending band of S1P in the same temperature interval (Fig. 5 *B*).

Slope changes may indicate a change in the aggregation behavior of S1P. We tested this possibility by examining the thermal dependence of the static light scattering of S1P aqueous suspensions in the temperature range close to 65°C. The data in Fig. 6 indicate a sharp decrease in static light-scattering intensity at 55°C. This would be compatible with a decrease in aggregate size corresponding to the observed thermal effects revealed by IR (at 65°C) and DSC (at 60°C). It is normal for this kind of thermal event to be detected at slightly different temperatures depending on the techniques used (19).

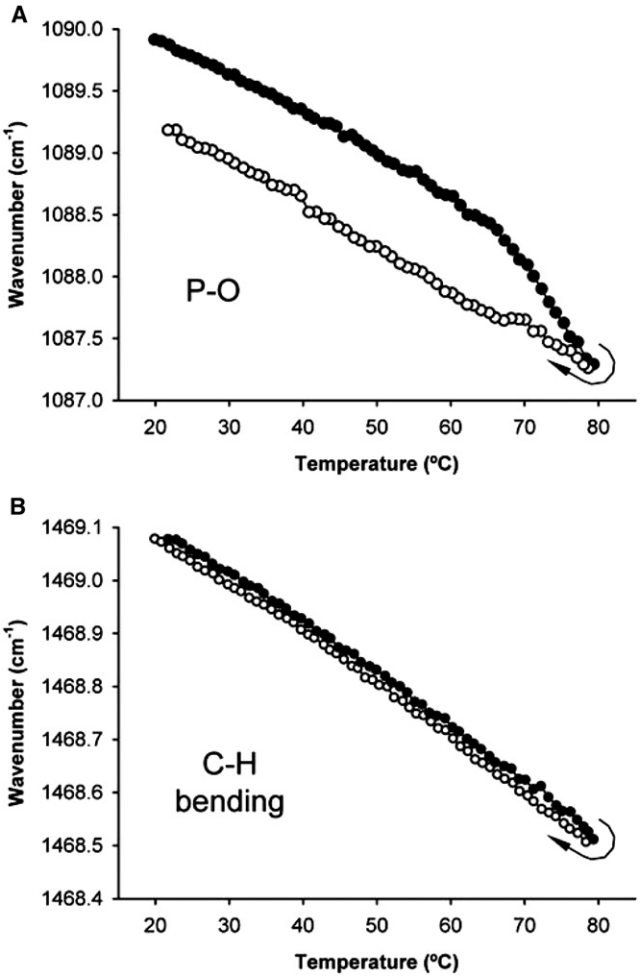

FIGURE 5 Band positions (maximal frequencies) of S1P vibrational bands as a function of temperature. (*A*) P-O stretching. (*B*) C-H bending. (•) Heating run. (○) Cooling run.

S1P in phospholipid bilayers

We first tested the effect of S1P on lipid bilayers by examining the behavior of S1P:DEPE mixtures using DSC. Pure DEPE displays a narrow endotherm centered at 37.5°C, corresponding to its gel-to-fluid phase transition. The presence of 5 mol % S1P (Fig. 7 *A*) produced a clear widening of the endotherm and a decrease of the area under it, i.e., the transition enthalpy. These effects became more evident with increasing proportions of S1P, together with a shift of the endotherm toward lower temperatures. At 10 mol % S1P and above, small ''shoulders'' are seen in the thermograms, which may suggest imperfect mixing of both lipids. These shoulders did not disappear with further heating and cooling of the samples, and they were too small to allow (or even justify) the use of a signal decomposition procedure. The midpoint transition temperatures, transition enthalpies, and widths at midheight of the thermograms are plotted in Fig. 8, *A–C*, as a function of S1P concentration in the bilayer. Note, however, that the S1P effects were quantitatively small; even at 50 mol %, the DEPE transition was clearly visible. Essentially similar results were obtained when mixtures of S1P and DPPC were examined by DSC (data not shown).

DEPE has the interesting property of displaying both a gel-fluid and a lamellar-hexagonal transition within a convenient range of temperatures. The lamellar-hexagonal phase transition occurs at ~65°C. The effects of S1P on this thermotropic transition are shown in Fig. 7 *B*. Even relatively small amounts of S1P (e.g., 5 mol %) drastically modify the transition endotherm, shifting it to higher temperatures and greatly decreasing the transition enthalpy. The endotherm becomes hardly detectable at S1P concentrations beyond 10 mol %. The thermodynamic parameters corresponding to the endotherms in Fig. 7 *B* are plotted versus S1P concentration in Fig. 8, *D–F*.

A partial phase diagram for the S1P/DEPE system in excess water (Fig. 9) was constructed on the basis of DSC thermograms as shown in Fig. 7. S1P appears to mix well with DEPE in the gel phase, as shown by the gradual decrease of the onset temperature of gel melting. Moreover, S1P increases the completion temperature of the lamellar-hexagonal

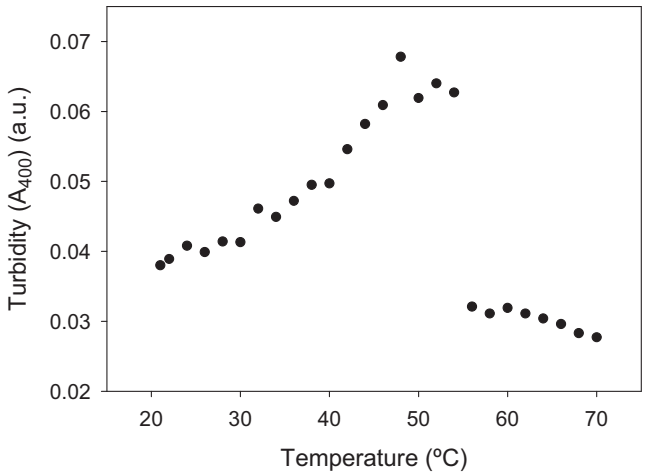

FIGURE 6 Static light scattering of a 1 mM S1P dispersion in buffer, as a function of temperature.

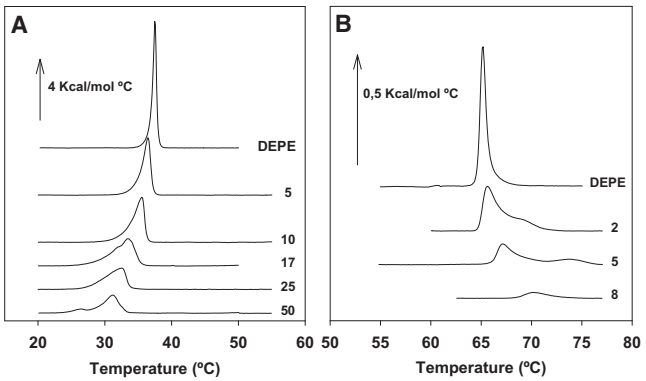

FIGURE 7 Phase transitions of pure DEPE and DEPE:S1P mixtures as detected by DSC. (*A*) Gel-fluid transitions. (*B*) Lamellar-hexagonal transitions. Second heating scans. The figures at the right side of each thermogram correspond to the S1P contents, in mole percentages.

transition in the region (up to 10 mol % S1P) where this transition is detectable by DSC. The presence of lamellar gel (L_β), lamellar fluid (L_α), and inverted hexagonal (H_{II}) phases in the regions of the phase diagram indicated in Fig. 9 were confirmed by ^{31}P-NMR spectra as shown in Fig. 10. For a sample containing 8 mol % S1P in DEPE, at 25°C, the wide asymmetric signal with a low-field shoulder is characteristic of the L_β phase. The gel-fluid transition is marked by a clear narrowing of the spectral line, as seen at 50°C. Finally, the spectrum at 80°C with a high-field shoulder is typical of the inverted hexagonal phase (20). ^{31}P-NMR spectra for a sample containing 50 mol % S1P in DEPE (i.e., corresponding to the right-hand part of the phase diagram in Fig. 9) are also shown in Fig. 10. At 30°C the spectrum has a width intermediate between those of the L_β and L_α phases, probably reflecting the coexistence of both. At 50°C the predominantly lamellar spectrum shows a clear H_{II} component. As seen in the DSC thermogram (Fig. 7), S1P gradually blurs the cooperativity of the L_α,-H_{II} transition, with the result that most of the phase diagram is occupied by coexisting L_α and H_{II} phases. Then, at 80°C the ^{31}P-NMR spectrum (Fig. 10) corresponds to a pure H_{II} phase. In most ^{31}P-NMR spectra, some narrow, isotropic components near 0 ppm are seen, probably corresponding to monomeric S1P in solution (see Fig. 1). In

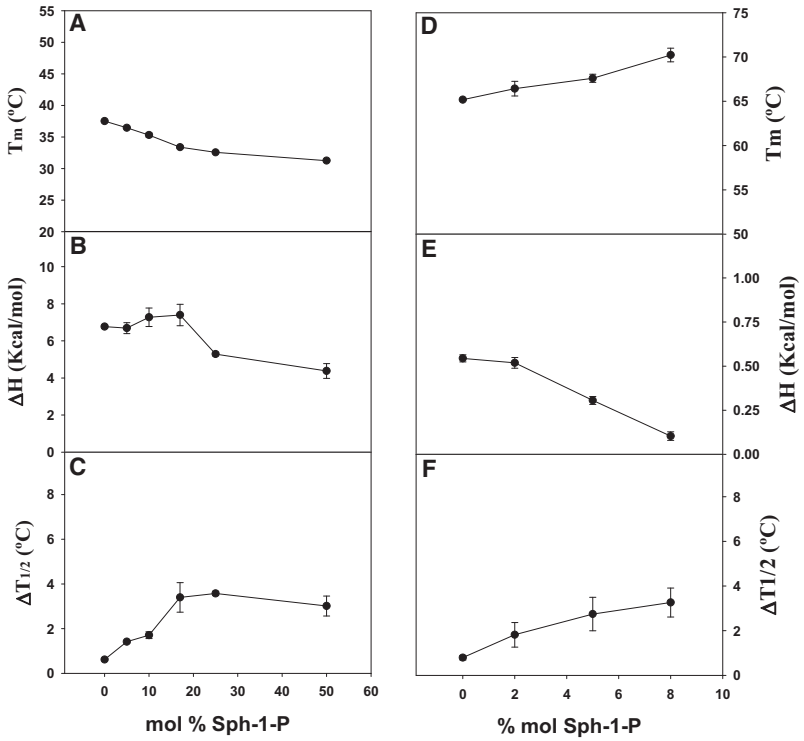

FIGURE 8 Thermodynamic parameters of the phase transitions of pure DEPE and DEPE:S1P mixtures. Data are derived from thermograms as shown in Fig. 6. (*A–C*) Gel-fluid transitions. (*D–F*) Lamellar-hexagonal transitions. (*A* and *D*) Midpoint transition temperatures. (*B* and *E*) Transition enthalpies. (*C* and *F*) Transition widths at midheight of the thermograms.

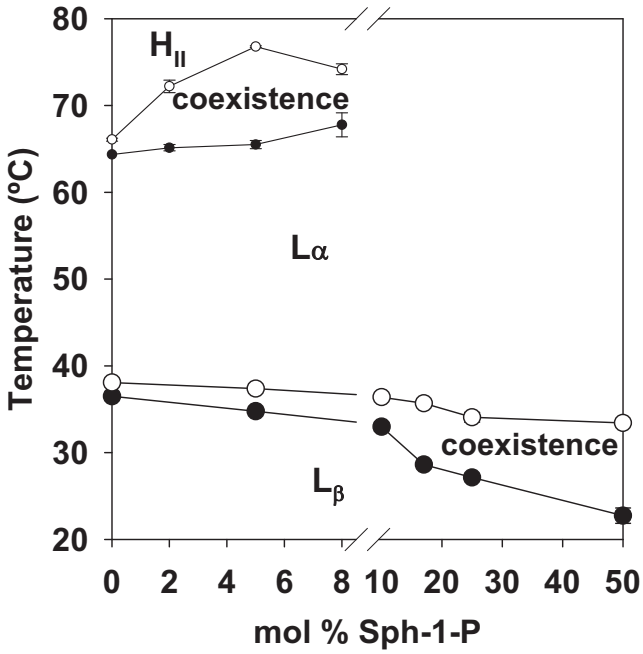

FIGURE 9 Temperature-composition diagram (''phase diagram'') for the DEPE:S1P system in excess water. Experimental data were derived from DSC data as shown in Fig. 7. L_β, lamellar gel phase. L_α, lamellar fluid, or liquid crystalline phase. H_{II}, inverted hexagonal phase. Regions of coexisting domains are marked ''coexistence''.

summary, S1P appears to be a potent stabilizer of the lamellar phase formed by DPPE, at the expense of the hexagonal phase, and a fluidizer of the lamellar phase.

A further view of the effect of S1P on phospholipid bilayers can be obtained by IR spectroscopy, particularly when a perdeuterated-chain phospholipid is used so that the CH_2 and CD_2 vibrations of the sphingolipid and the glycerophospholipid can be separately observed. The results corresponding to a S1P/d_{62}-DPPC equimolar mixture are shown in Fig. 11.

A plot corresponding to the symmetric stretching of the CD_2 bands of d_{62}-DPPC is shown in Fig. 11 *A* for pure d_{62}-DPPC and for an equimolar mixture, S1P:d_{62}-DPPC. The only effect of S1P was to decrease the transition temperature by ~6°C, in agreement with the DSC measurements. Exactly the same result was deduced from measurements of asymmetric CD_2 vibrations (not shown).

The CO stretching vibration band of d_{62}-DPPC is also sensitive to the gel-fluid phase transition (21) (note that S1P lacks any CO group). The position of the CO band of the glycerophospholipid is plotted as a function of temperature in Fig. 11 *B* for both pure d_{62}-DPPC and an equimolar S1P:d_{62}-DPPC mixture. S1P had a clear effect of shifting the position of the CO vibration band by ~+2 wavenumbers at all temperatures. The shift is certainly an indication of molecular interactions occurring between S1P and the phospholipid at the bilayer-water interface level. Moreover, the DPPC CO band also reflects the decrease in gel-fluid transition temperature caused by the presence of S1P in the bilayers. Deconvoluted contours of the C=0 stretching band above and below the gel-fluid transition temperature of DPPC are shown in Fig. 12. The deconvoluted band exhibits a broad and asymmetric shape. Two components that arise from different hydration levels of the carbonyl group are clearly visible, with the high-frequency component corresponding to a subpopulation of free C=0, and the low-frequency one to an H-bonded subpopulation (21–23). The presence of S1P increases the relative intensity of the low-frequency (i.e., high wavenumber) component, suggesting that the sphingolipid increases the level of hydration of the phospholipid carbonyl group, thus shifting the C=0 stretching band toward higher wavenumbers (Fig. 12).

Fig. 11 *C* shows the thermal behavior of the symmetric CH_2 vibration bands of S1P when it is incorporated into a perdeuterated DPPC bilayer. At variance with the pure S1P, the hydrocarbon chain of S1P in the mixture appears to become slightly more disordered above 55°C. This probably corresponds to the region in the phase diagram where the H_{II} phase becomes predominant (Fig. 10, *E* and *F*). L_α-H_{II} transitions are known to cause disordering of lipid chains (25).

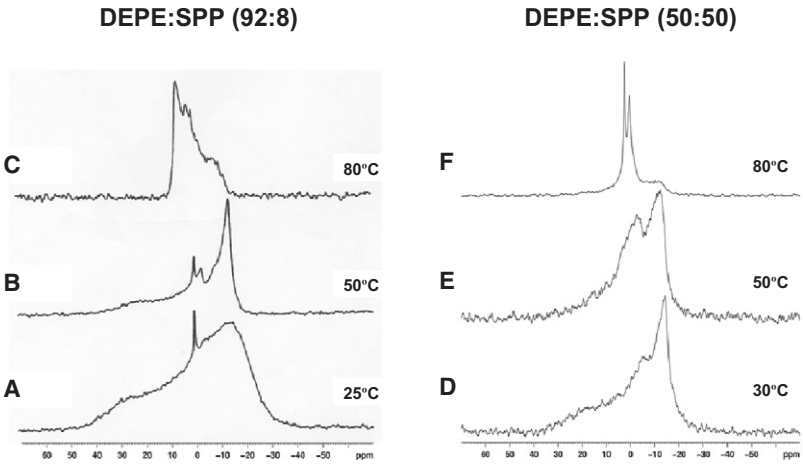

FIGURE 10 ^{31}P-NMR spectra of DEPE:S1P mixtures in excess water, as a function of temperature. Temperatures are indicated at the right-hand side for each spectrum.

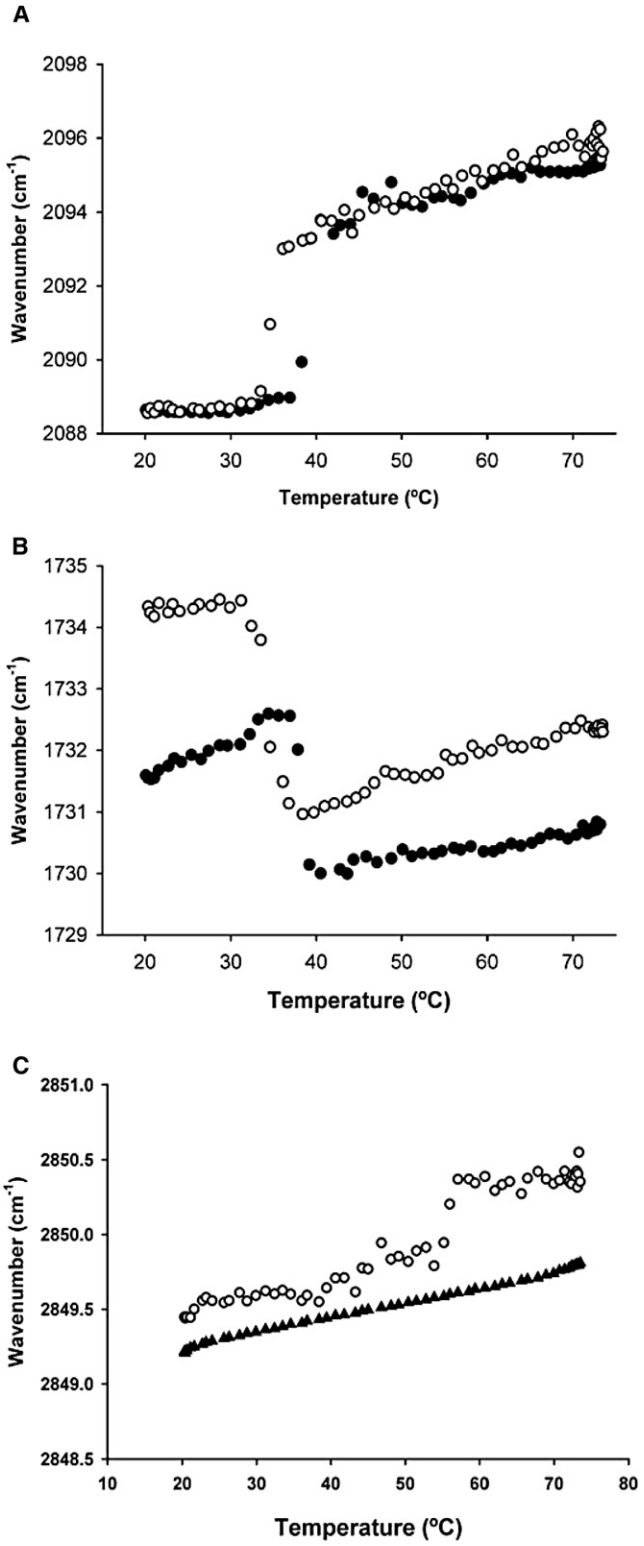

FIGURE 11 The gel-fluid transitions of pure d_{62}-DPPC, pure S1P, and d_{62}-DPPC:S1P mixtures as detected by IR spectroscopy. The maximal frequencies (band positions) of the corresponding bands are plotted as a function of temperature (data from the second heating scan). (*A*) C-D symmetric stretching vibrations of d_{62}-DPPC. (*B*) CO stretching vibrations of d_{62}-DPPC. (*C*) C-H symmetric stretching vibrations of S1P. (●) Pure d_{62}-DPPC. (○) d_{62}-DPPC:S1P mixture at a 1:1 mol ratio. (▲) Pure S1P.

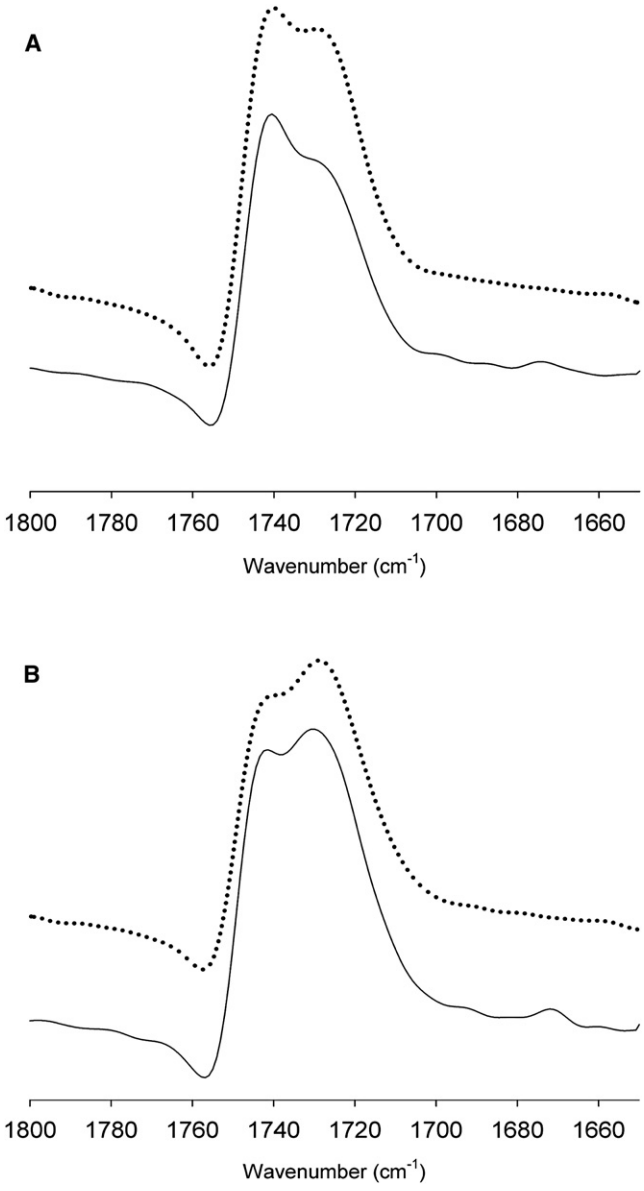

FIGURE 12 C=0 stretching region of the deconvoluted d_{62} DPPC IR spectrum. Dotted line: Pure d_{62}-DPPC. Continuous line: d_{62}-DPPC:S1P mixture at a 1:1 mol ratio. (*A*) 25°C. (*B*) 50°C. Deconvolution parameters: bandwidth = 18, enhancement factor = 2.

DISCUSSION

Physical data

S1P is an amphiphile whose polar moiety is formed by a phosphate esterified to the C1 OH, by the C2 amino, and by the C3 hydroxy groups of sphingosine. The nonpolar part of S1P corresponds to the 15-carbon chain of sphingosine. In this sense, the molecule is somewhat similar to other ''single-chain'' lipids whose behavior in membranes has been studied in detail, such as lysophosphatidylcholine (26,27), palmitoylcarnitine (21,28), ''platelet activating factor'' (29), edelfosine (30), and the sphingolipid *N*-acylsphingosine, or C_2-ceramide

(31). S1P shares with these ''single-chain'' lipids the property of having a monomer-micelle transition in the micromolar range (Fig. 1). Consequently, as with any other soluble amphiphile in the presence of membranes, S1P will exist in equilibrium between the aqueous and membranous compartments because the concentration of S1P in the aqueous compartment is close to its CMC (32).

The effects of S1P on the gel-fluid transition of DEPE or DPPC are moderate from a quantitative point of view. The data in Figs. 7–9 are compatible with a molecule that inserts and orients itself in the bilayer in parallel with the glycerophospholipid acyl chains. There is an interaction with the CO group of the host lipids (Fig. 11 *B*) that could reasonably consist of an increased level of hydration of the said CO group. The data in Fig. 4 and 11 *C* inform us that the S1P alkyl chain appears to be quite highly ordered when in the pure form, and it remains equally ordered when inserted in the DPPC bilayer. Figs. 7 and 11 *A* show that S1P is fluidifying the glycerophospholipid molecules, thus decreasing the bilayer transition temperature. This is remarkable, since the order-disorder transition temperature of pure aqueous S1P is 65.0°C, i.e., higher than that of pure DEPE. This would, in principle, lead to the mixture having a transition temperature higher than pure DEPE. The fact that the opposite is found may be the result of specific DEPE-S1P interactions, as revealed, e.g., by the data in Fig. 11 *B*.

The IR and DSC data concur in showing that the influence of S1P on phospholipid bilayers is qualitatively and quantitatively comparable to that of the structurally similar palmitoylcarnitine (21,28). An ether analog of lysophosphatidylcholine behaved very much like S1P in the calorimetric measurements (26), whereas egg lysophosphatidylcholine departed from this pattern, first increasing and then decreasing only at mole fractions above 0.3 the transition temperature of DPPC (27). By comparing the effects of S1P with those of other sphingolipids, it can be stated that DEPE-S1P mixtures behave, from the point of view of the gel-fluid transition, in an intermediate way between those containing C_2 and C_6 ceramides (*N*-acetylsphingosine and *N*-hexanoylsphingosine, respectively) (31).

S1P modifies in a more drastic way the lamellar-to-inverted hexagonal phase transition of DEPE. The main effect of S1P is to counter this transition, stabilizing the lamellar phase. This is particularly evident at <10 mol % S1P, when the L-H calorimetric endotherm is still detectable (Figs. 7 *B* and 9). The most likely explanation for this behavior is the geometry of the S1P molecule, whose cross section would be larger at the headgroup than at the nonpolar end, thus making S1P a ''conically shaped'' amphiphile. Such conical molecules tend to favor the ''positive curvature'' of the monolayers (33), correspondingly opposing the negative curvature adopted by the monolayers in the inverted phases. Similar molecules (e.g., lysophosphatidylcholine) have equally been shown to hinder the formation of inverted phases (34). Equally, palmitoylcarnitine behaved in a very similar way to S1P when the lamellar-hexagonal transition of DEPE was tested in the presence of that amphiphile by DSC (28) or IR (21), and the same is true of the geometrically related *N*-acetylsphingosine (31). Conversely, long-chain ceramides with an ''inverted-cone'' shape were found to facilitate the lamellar-hexagonal transition of phosphatidylethanolamines (31,35). Also in contrast to S1P, sphingosine has a small effect on the L-H transition of DEPE, facilitating to some extent the inverted hexagonal phase formation at mole ratios of 0–20 mol % (36,37).

Physiological implications

S1P is a lipid that is synthesized within the cell membrane. As we discussed previously for ceramides (12), S1P action may occur either by binding a specific site in a protein, or by changing certain membrane properties. However, an important difference between S1P and ceramide (31), sphingosine (36), or ceramide-1-phosphate (38) is that S1P is a soluble amphiphile with a well-defined CMC (Fig. 1), whereas the other three are totally insoluble. This may be significant because micromolar concentrations of S1P can exist free in the cytosol, enabling it to interact with soluble enzymes. S1P exerts many of its physiological effects at submicromolar concentrations (1). Moreover, in the absence of specific biochemical data, the results presented here provide the physical basis for a putative S1P effect through changes in the membrane physical properties, in particular the stabilization of the lamellar structure versus negatively curved, inverted phases. An increasing number of membrane enzymes have been found that are sensitive not so much to the actual lipid phase (since, at equilibrium, membrane lipids always exist in the lamellar phase), but to the propensity of the bilayer to adopt a negatively curved, inverted phase (39–42). S1P would, according to our data, decrease any propensity toward inverted phase formation.

Various data from the literature can be interpreted in the light of these observations. Li et al. (43) described the induction of endocytic vesicles by ceramide in fibroblasts, whereas S1P was found to be inactive in this respect. Vesicle fission and fusion can be induced by ceramide because of its ''inverted conical'' shape (i.e., a headgroup larger than the tail cross section) (33) and consequent tendency to favor inverted phases (44–46). S1P would be inactive inducing endocytosis because of its ''conical shape'' and corresponding tendency to stabilize lamellar versus inverted phases. S1P was found to mimic, albeit with a smaller activity, several effects of the isomorphic lysophosphatidic acid (47). Also noteworthy in this aspect is the observed suppression of ceramide-mediated apoptosis by S1P (2,5), an example of two sphingolipids with contrasting shapes and opposite physiological effects. Thus the biophysical data appear to reveal what we believe is a novel aspect of what has been called the ''sphingolipid rheostat'', or the physiological balance between ceramide and S1P (5,48,49).

A final point concerns the paradox that although substantial amounts of S1P are required to observe any physical changes in membranes (cf. our data), only very small proportions of this lipid appear to exist in cell membranes. As we previously discussed regarding diacylglycerol (50), the solution to this problem probably lies in the localized formation of lipid signals (e.g., diacylclycerol, ceramide, and S1P) at a given time in a given membrane microdomain. In this way, high local concentrations of second messengers can be produced while very low average concentrations of those messengers are maintained.

The authors are indebted to Dr. A. Gómez-Muñoz for his guidance on the physiological effects of S1P.

This work was supported in part by grants from Fundación Areces, Ministerio de Educación y Ciencia (BFU 2008-01637), the Basque Government (Etortek 07/26), and the University of the Basque Country (GIU 06/42). M.G.P. was supported by the Ministerio de Educación y Ciencia.

REFERENCES

1. Kim, R. H., K. Takabe, S. Milstien, and S. Spiegel. 2009. Export and functions of sphingosine-1-phosphate. *Biochim. Biophys. Acta.* 1791: 692–696.
2. Taha, T. A., T. D. Mullen, and L. M. Obeid. 2006. A house divided: ceramide, sphingosine, and sphingosine-1-phosphate in programmed cell death. *Biochim. Biophys. Acta.* 1758:2027–2036.
3. Donati, C., and P. Bruni. 2006. Sphingosine 1-phosphate regulates cytoskeleton dynamics: implications in its biological response. *Biochim. Biophys. Acta.* 1758:2037–2048.
4. Olivera, A., and S. Spiegel. 1993. Sphingosine-1-phosphate as second messenger in cell proliferation induced by PDGF and FCS mitogens. *Nature.* 365:557–560.
5. Ader, I., B. Malavaud, and O. Cuvillier. 2009. When the sphingosine kinase 1/sphingosine-1phosphate pathway meets hypoxia signalling: new targets for cancer therapy. *Cancer Res.* 69:3723–3726.
6. Cuvillier, O., G. Pirianov, B. Kleuser, P. G. Vanek, O. A. Coso, et al. 1996. Suppression of ceramide-mediated programmed cell death by sphingosine-1-phosphate. *Nature.* 381:800–803.
7. Brizuela, L., M. Rábano, P. Gangoiti, N. Narbona, J. M. Macarulla, et al. 2007. Sphingosine-1-phosphate stimulates aldosterone secretion through a mechanism involving the PI3K/PKB and MEK/ERK 1/2 pathways. *J. Lipid Res.* 48:2264–2274.
8. Rosen, H., P. J. González-Cabrera, M. G. Sanna, and S. Brown. 2009. Sphingosine-1-phosphate receptor signaling. *Annu. Rev. Biochem.* 78: 743–768.
9. Means, C. K., and J. H. Brown. 2009. Sphingosine-1-phosphate receptor signalling in the heart. *Cardiovasc. Res.* 82:193–200.
10. Marsolais, D., and H. Rosen. 2009. Chemical modulators of S1P receptors as barrier-oriented therapeutic molecules. *Nat. Rev. Drug Discov.* 8:297–307.
11. Brownlee, C. 2001. Intracellular signalling: sphingosine-1-phosphate branches out. *Curr. Biol.* 11:535–538.
12. Kolesnick, R. N., F. M. Goñi, and A. Alonso. 2000. Compartmentalization of ceramide signaling: physical foundations and biological effects. *J. Cell. Physiol.* 184:285–300.
13. Arrondo, J. L., and F. M. Goñi. 1998. Infrared studies of protein-induced perturbation of lipids in lipoproteins and membranes. *Chem. Phys. Lipids.* 96:53–68.
14. Sot, J., F. M. Goñi, and A. Alonso. 2005. Molecular associations and surface-active properties of short- and long-*N*-acyl chain ceramides. *Biochim. Biophys. Acta.* 1711:12–19.
15. Sasaki, H., H. Arai, M. J. Cocco, and S. H. White. 2009. pH dependence of sphingosine aggregation. *Biophys. J.* 96:2727–2733.
16. Chapman, D., R. M. Williams, and B. D. Ladbrooke. 1967. Physical studies of phospholipids VI. Thermotropic and lyotropic mesomorphism of some 1,2-diacyl phosphatidylcholines (lecithins). *Chem. Phys. Lipids.* 1:445–475.
17. Mantsch, H. H., and R. N. McElhaney. 1991. Phospholipid phase transitions in model and biological membranes as studied by infrared spectroscopy. *Chem. Phys. Lipids.* 57:213–226.
18. Cortijo, M., A. Alonso, J. C. Gomez-Fernandez, and D. Chapman. 1982. Intrinsic protein-lipid interactions. Infrared spectroscopic studies of gramicidin A, bacteriorhodopsin and Ca^{2+}-ATPase in biomembranes and reconstituted systems. *J. Mol. Biol.* 157:597–618.
19. Kaschny, P., and F. M. Goñi. 1993. Spectroscopic properties of hydrophobic dyes incorporated into phospholipid bilayers. An application to the study of membrane-surfactant interactions. *J. Colloid Interface Sci.* 161:24–30.
20. Cullis, P. R., and B. de Kruijff. 1979. Lipid polymorphism and the functional roles of lipids in biological membranes. *Biochim. Biophys. Acta.* 559:399–420.
21. Echabe, I., M. A. Requero, F. M. Goñi, J. L. Arrondo, and A. Alonso. 1995. An infrared investigation of palmitoyl-coenzyme A and palmitoylcarnitine interaction with perdeuterated-chain phospholipid bilayers. *Eur. J. Biochem.* 231:199–203.
22. Blume, A., W. Hübner, and G. Messner. 1988. Fourier transform infrared spectroscopy of $^{13}C{=}O$-labeled phospholipids hydrogen bonding to carbonyl groups. *Biochemistry.* 27:8239–8249.
23. Lewis, R. N., R. N. McElhaney, W. Pohle, and H. H. Mantsch. 1994. Components of the carbonyl stretching band in the infrared spectra of hydrated 1,2-diacylglycerolipid bilayers: a reevaluation. *Biophys. J.* 67:2367–2375.
24. Reference deleted in proof.
25. Castresana, J., J. L. Nieva, E. Rivas, and A. Alonso. 1992. Partial dehydration of phosphatidylethanolamine phosphate groups during hexagonal phase formation, as seen by I.R. spectroscopy. *Biochem. J.* 282:467–470.
26. Blume, A., B. Arnold, and H. U. Weltzien. 1976. Effects of a synthetic lysolecithin analog on the phase transition of mixtures of phosphatidylethanolamine and phosphatidylcholine. *FEBS Lett.* 61:199–202.
27. Alonso, A., and F. M. Goñi. 1983. Effects of detergents and fusogenic lipids on phospholipid phase transitions. *J. Membr. Biol.* 71:183–187.
28. Veiga, M. P., M. A. Requero, F. M. Goñi, and A. Alonso. 1996. Effect of long-chain acyl-CoAs and acylcarnitines on gel-fluid and lamellar-hexagonal phospholipid phase transitions. *Mol. Membr. Biol.* 13:165–172.
29. Salgado, J., J. Villalain, and J. C. Gomez-Fernandez. 1993. Effects of platelet-activating factor and related lipids on dielaidoylphosphatidylethanolamine by DSC, FTIR and NMR. *Biochim. Biophys. Acta.* 1145:284–292.
30. Busto, J. V., J. Sot, F. M. Goni, F. Mollinedo, and A. Alonso. 2007. Surface-active properties of the antitumour ether lipid 1-*O*-octadecyl-2-*O*-methyl-rac-glycero-3-phosphocholine (edelfosine). *Biochim. Biophys. Acta.* 1768:1855–1860.
31. Sot, J., F. J. Aranda, M. I. Collado, F. M. Goni, and A. Alonso. 2005. Different effects of long- and short-chain ceramides on the gel-fluid and lamellar-hexagonal transitions of phospholipids: a calorimetric, NMR, and x-ray diffraction study. *Biophys. J.* 88:3368–3380.
32. Lichtenberg, D. 2000. Phase boundaries in mixtures of membrane-forming amphiphiles and micelle-forming amphiphiles. *Biochim. Biophys. Acta.* 1508:1–19.
33. Helfrich, W. 1973. Elastic properties of lipid bilayers: theory and possible experiments. *Z. Naturforsch. [C].* 28(C):693–703.
34. Basáñez, G., F. M. Goñi, and A. Alonso. 1998. Effect of single chain lipids on phospholipase C-promoted vesicle fusion. A test for the stalk hypothesis of membrane fusion. *Biochemistry.* 37:3901–3908.

35. Veiga, M. P., J. L. Arrondo, F. M. Goñi, and A. Alonso. 1999. Ceramides in phospholipid membranes: effects on bilayer stability and transition to nonlamellar phases. *Biophys. J.* 76:342–350.

36. Contreras, F. X., J. Sot, A. Alonso, and F. M. Goñi. 2006. Sphingosine increases the permeability of model and cell membranes. *Biophys. J.* 90:4085–4092.

37. López García, F., J. Villalin, and J. C. Gómez-Fernández. 1994. A phase behaviour study of mixtures of sphingosine with zwiterionic phospholipids. *Biochim. Biophys. Acta.* 1194:281–288.

38. Kooijman, E. E., J. Sot, L. R. Montes, A. Alonso, A. Gericke, et al. 2008. Membrane organization and ionization behaviour of the minor but crucial lipid ceramide-1-Phosphate. *Biophys. J.* 94:4320–4330.

39. Epand, R. M. 1985. Diacylglycerols, lysolecithin, or hydrocarbons markedly alter the bilayer to hexagonal phase transition temperature of phosphatidylethanolamines. *Biochemistry.* 24:7092–7095.

40. Cornell, R. B., and R. S. Arnold. 1996. Modulation of the activities of enzymes of membrane lipid metabolism by non-bilayer-forming lipids. *Chem. Phys. Lipids.* 81:215–227.

41. Goñi, F. M., G. Basáñez, M. B. Ruiz-Argüello, and A. Alonso. 1998. Interfacial enzyme activation, non-lamellar phase formation and membrane fusion. Is there a conducting thread? *Faraday Discuss.* 111:55–78.

42. Halperin, A., and O. G. Mouritsen. 2005. Role of lipid protrusions in the function of interfacial enzymes. *Eur. Biophys. J.* 34:967–971.

43. Li, R., E. J. Blanchette-Mackie, and S. Ladisch. 1999. Induction of endocytic vesicles by exogenous C(6)-ceramide. *J. Biol. Chem.* 274: 21121–21127.

44. Ruiz-Argüello, M. B., F. M. Goñi, and A. Alonso. 1998. Vesicle membrane fusion induced by the concerted activities of sphingomyelinase and phospholipase C. *J. Biol. Chem.* 273:22977–22982.

45. Holopainen, J. M., J. Y. Lehtonen, and P. K. Kinnunen. 1997. Lipid microdomains in dimyristoylphosphatidylcholine-ceramide liposomes. *Chem. Phys. Lipids.* 88:1–13.

46. Holopainen, J. M., M. Subramanian, and P. K. Kinnunen. 1998. Sphingomyelinase induces lipid microdomain formation in a fluid phosphatidylcholine/sphingomyelin membrane. *Biochemistry.* 37:17562–17570.

47. Gueguen, G., B. Gaigé, J. M. Grévy, P. Rogalle, J. Bellan, et al. 1999. Structure-activity analysis of the effects of lysophosphatidic acid on platelet aggregation. *Biochemistry.* 38:8440–8450.

48. Maceyka, M., S. G. Payne, S. Milstien, and S. Spiegel. 2002. Sphingosine kinase, sphingosine-1-phosphate, and apoptosis. *Biochim. Biophys. Acta.* 1585:193–201 (Review).

49. Lavieu, G., F. Scarlatti, G. Sala, T. Levade, R. Ghidoni, et al. 2007. Is autophagy the key mechanism by which the sphingolipid rheostat controls the cell fate decision? *Autophagy.* 3:45–47 (Review).

50. Goñi, F. M., and A. Alonso. 1999. Structure and functional properties of diacylglycerols in membranes. *Prog. Lipid Res.* 38:1–48.